# 18 Electronic Excitation Energies of Molecular Systems from the Bethe–Salpeter Equation
## *Example of the $H_2$ Molecule*

*Elisa Rebolini, Julien Toulouse, and Andreas Savin*

**CONTENTS**



## 18.1 INTRODUCTION

Time-dependent density functional theory (TDDFT)[1] within the linear response formalism[2–4] is nowadays the most widely used approach to the calculation of electronic excitation energies of molecules and solids. Applied within the adiabatic approximation and with the usual local or semilocal density functionals, TDDFT

gives indeed in many cases excitation energies with reasonable accuracy and low computational cost. However, several serious limitations of these approximations are known, for example, for molecules, too low charge-transfer excitation energies,[5] lack of double excitations,[6] and wrong behavior of the excited-state surface along a bond-breaking coordinate (see, e.g., reference [7]). Several remedies to these problems are actively being explored, including long-range corrected TDDFT,[8, 9] which improves charge-transfer excitation energies; dressed TDDFT,[6, 10, 11] which includes double excitations; and time-dependent density-matrix functional theory (TDDMFT),[12–16] which tries to address all these problems.

In the condensed-matter physics community, the Bethe–Salpeter equation (BSE) applied within the GW approximation (see, e.g., references [17–19]) is often considered as the most successful approach to overcome the limitations of TDDFT. Although it has been often used to describe excitons (bound electron-hole pair) in periodic systems, it is also increasingly applied to calculations of excitation energies in finite molecular systems.[20–31] In particular, the BSE approach is believed to give accurate charge-transfer excitation energies in molecules,[29, 31] and when used with a frequency-dependent kernel, it is in principle capable of describing double excitations.[32, 33]

In this work, we examine the merits of the BSE approach for calculating excitation energies of the prototype system of quantum chemistry, the $H_2$ molecule. The paper is organized as follows. In Section 18.2, we give a review of Green's function many-body theory. In Section 18.3, we give the general working equations for a BSE calculation within the static GW approximation in a finite spin-orbital basis and the corresponding spin-adapted expressions for closed-shell systems. In Section 18.4, we apply the equations to the $H_2$ molecule in a minimal basis and discuss the possibility of obtaining correct spin-singlet and spin-triplet excited-state energy curves as a function of the internuclear distance. Section 18.5 contains our conclusions. Hartree atomic units are used throughout.

## 18.2 REVIEW OF GREEN'S FUNCTION MANY-BODY THEORY

We start by giving a brief review of Green's function many-body theory for calculating excitation energies. For more details, see references [17], [19], and [34].

### 18.2.1 One-Particle Green's Function

Let $|N\rangle$ be the normalized ground-state wavefunction for a system of $N$ electrons described by the Hamiltonian $\hat{H}$. The time-ordered one-particle equilibrium Green's function is defined as

$$\begin{aligned} iG(1,2) &= \langle N \mid \hat{T}[\hat{\Psi}(1)\hat{\Psi}^{\dagger}(2)] \mid N\rangle \\ &= \theta(t_1 - t_2)\langle N \mid \hat{\Psi}(1)\hat{\Psi}^{\dagger}(2) \mid N\rangle - \theta(t_2 - t_1)\langle N \mid \hat{\Psi}^{\dagger}(2)\hat{\Psi}(1) \mid N\rangle. \end{aligned} \tag{18.1}$$

Index 1 stands for space, spin, and time coordinates $(\mathbf{r}_1,\sigma_1,t_1) = (\mathbf{x}_1,t_1)$. $\hat{T}$ is the Wick time-ordering operator that orders the operators with larger times on the left,

and θ is the Heaviside step function. The whole time dependence is contained in $\hat{\Psi}(1) = e^{i\hat{H}t_1}\hat{\Psi}(\mathbf{x}_1)e^{-i\hat{H}t_1}$ and $\hat{\Psi}^\dagger(2) = e^{i\hat{H}t_2}\hat{\Psi}^\dagger(\mathbf{x}_2)e^{-i\hat{H}t_2}$, which are the annihilation and creation field operators in the Heisenberg representation.

In the absence of external potential, the system is invariant under time translation; therefore, the Green's function depends only on $\tau = t_1 - t_2$. By introducing the closure relation for excited states with $N-1$ or $N+1$ particles, one can get

$$iG(\mathbf{x}_1,\mathbf{x}_2;\tau) = \theta(\tau)\sum_A \langle N \mid \hat{\psi}(\mathbf{x}_1) \mid N+1, A\rangle\langle N+1, A \mid \hat{\psi}^\dagger(\mathbf{x}_2) \mid N\rangle e^{-i(E_{N+1,A}-E_N)\tau} - \theta(-\tau)\sum_I \langle N \mid \hat{\psi}^\dagger(\mathbf{x}_2) \mid N-1, I\rangle\langle N-1, I \mid \hat{\psi}(\mathbf{x}_1) \mid N\rangle e^{-i(E_N-E_{N-1,I})\tau}, \tag{18.2}$$

where $E_N$, $E_{N+1,A}$, and $E_{N-1,I}$ are the energies of the ground state $|N\rangle$, the $A$th excited state with $N+1$ particles $|N+1,A\rangle$, and the $I$th excited state with $N-1$ particles $|N-1,I\rangle$, respectively. The Lehmann representation of the one-particle Green's function is obtained by Fourier transform

$$G(\mathbf{x}_1,\mathbf{x}_2;\omega) = \sum_A \frac{f_A(\mathbf{x}_1)f_A^*(\mathbf{x}_2)}{\omega - \mathcal{E}_A + i0^+} + \sum_I \frac{f_I(\mathbf{x}_1)f_I^*(\mathbf{x}_2)}{\omega - \mathcal{E}_I - i0^+}, \tag{18.3}$$

where $f_A(\mathbf{x}) = \langle N \mid \hat{\psi}(\mathbf{x}) \mid N+1, A\rangle$ and $f_I(\mathbf{x}) = \langle N-1, I \mid \hat{\psi}(\mathbf{x}) \mid N\rangle$ are the Dyson orbitals, and $\mathcal{E}_A = E_{N+1,A} - E_N$ and $\mathcal{E}_I = E_N - E_{N-1,I}$ are minus the electron affinities and ionization energies, respectively.

### 18.2.2 Two-Particle Green's Function

The time-ordered two-particle Green's function is defined as

$$i^2G_2(1,2;1',2') = \langle N \mid \hat{T}[\hat{\Psi}(1)\hat{\Psi}(2)\hat{\Psi}^\dagger(2')\hat{\Psi}^\dagger(1')] \mid N\rangle. \tag{18.4}$$

Depending on the time ordering, it describes the propagation of a pair of holes, of electrons, or of a hole and an electron. In the case of optical absorption, one is only interested in the propagation of a hole-electron pair.

Let χ be the four-point polarizability,

$$\chi(1,2;1',2') = iG_2(1,2;1',2') - iG(1,1')\,G(2,2'). \tag{18.5}$$

It describes the coupled motion of two particles minus the motion of the independent ones. When the times are appropriately ordered, the four-point polarizability reduces to the linear response function

$$\chi(\mathbf{x}_1,\mathbf{x}_2;\mathbf{x}_1',\mathbf{x}_2';\tau) = \chi(\mathbf{x}_1,t_1,\mathbf{x}_2,t_2;\mathbf{x}_1',t_1^+,\mathbf{x}_2',t_2^+), \tag{18.6}$$

where $t_1^+ = t_1 + 0^+$. The Lehmann representation of the response function explicitly gives the excitation energies as poles in ω,

$$\chi\left(\mathbf{x}_1,\mathbf{x}_2;\mathbf{x}_1',\mathbf{x}_2';\omega\right) = \sum_{K\neq 0}\frac{\left\langle N\left|\hat{\Psi}^\dagger\left(\mathbf{x}_1'\right)\hat{\Psi}(\mathbf{x}_1)\right|N,K\right\rangle\left\langle N,K\left|\hat{\Psi}^\dagger\left(\mathbf{x}_2'\right)\hat{\Psi}(\mathbf{x}_2)\right|N\right\rangle}{\omega-(E_{N,K}-E_N)+i0^+} - \sum_{K\neq 0}\frac{\left\langle N\left|\hat{\Psi}^\dagger\left(\mathbf{x}_2'\right)\hat{\Psi}(\mathbf{x}_2)\right|N,K\right\rangle\left\langle N,K\left|\hat{\Psi}^\dagger\left(\mathbf{x}_1'\right)\hat{\Psi}(\mathbf{x}_1)\right|N\right\rangle}{\omega+(E_{N,K}-E_N)-i0^+}, \tag{18.7}$$

where $|N,K\rangle$ is the $K$th excited state with $N$ particles of energy $E_{N,K}$. The ground state $|N,0\rangle = |N\rangle$ is excluded from the sum. It is also useful to define the independent-particle (IP) polarizability $\chi_{IP}(1,2;1',2') = -iG(1,2')G(2,1')$. Its Lehmann representation is easily obtained by calculating $\chi_{IP}\left(\mathbf{x}_1,\mathbf{x}_2;\mathbf{x}_1',\mathbf{x}_2';\tau\right) = -iG\left(\mathbf{x}_1,\mathbf{x}_2';\tau\right)G\left(\mathbf{x}_2,\mathbf{x}_1';-\tau\right)$ with Equation 18.2 and taking the Fourier transform

$$\chi_{IP}(\mathbf{x}_1,\mathbf{x}_2;\mathbf{x}_1',\mathbf{x}_2';\omega) = \sum_{IA}\frac{f_I^*(\mathbf{x}_1')f_A(\mathbf{x}_1)f_A^*(\mathbf{x}_2')f_I(\mathbf{x}_2)}{\omega-(\mathcal{E}_A-\mathcal{E}_I)+i0^+} - \sum_{IA}\frac{f_I^*(\mathbf{x}_2')f_A(\mathbf{x}_2)f_A^*(\mathbf{x}_1')f_I(\mathbf{x}_1)}{\omega+(\mathcal{E}_A-\mathcal{E}_I)-i0^+}. \tag{18.8}$$

In practice, the one- and two-particle Green's function can be calculated with equations of motion.

### 18.2.3 Dyson Equation

To make easier the connection with expressions in a finite spin-orbital basis, we systematically use four-point indexes for all the two-electron quantities. The starting point is therefore a fully nonlocal time-dependent Hamiltonian

$$\hat{H}(t_1) = \int d\mathbf{x}_1 d1'\hat{\Psi}^\dagger(1)h(1,1')\hat{\Psi}(1') + \frac{1}{2}\int d\mathbf{x}_1 d2 d1' d2'\hat{\Psi}^\dagger(1)\hat{\Psi}^\dagger(2)v(1,2;1',2')\hat{\Psi}(1')\hat{\Psi}(2'), \tag{18.9}$$

where $v(1,2;1',2') = v_{ee}(|\mathbf{r}_1 - \mathbf{r}_2|)\delta(t_1,t_2)\delta(1,1')\delta(2,2')$ is the spin-independent instantaneous Coulomb electron–electron interaction, and $h(1,1')$ is the one-electron Hamiltonian that contains the electron kinetic operator and the nuclei–electron interaction $V_{ne}$

$$h(1,1') = -\delta(1,1')\frac{\overset{2}{\nabla}_1}{2} + \delta(1,1')V_{ne}(\mathbf{r}_1). \tag{18.10}$$

Using the equations of motion for the Heisenberg creation and annihilation operators in the expression of the derivative of $G$ with respect to time,[17] one can obtain the following equation:

$$i\int d3\delta(1,3)\frac{\partial}{\partial t_1}G(3,2)-\int d3h(1,3)G(3,2) + i\int d3d1'd3'v(1,3;1',3')G_2(1',3'^{+};2,3^{++})=\delta(1,2), \tag{18.11}$$

where $^{++}$ stands for $t_3^+ + 0^+$. A whole series of equations can be derived for the Green's functions, relating the one-particle Green's function to the two-particle Green's function, the two-particle Green's function to the three-particle Green's function, etc. However, solving this set of equations is not wanted.

To avoid this, one can use the Schwinger derivative technique. Introducing an external time-dependent potential $U(1,1') = U(\mathbf{x}_1,\mathbf{x}_1',t_1)\delta(t_1,t_1')$, one can express the two-particle Green's function in terms of the one-particle Green's function and its derivative with respect to $U$, evaluated at $U = 0$:

$$\frac{\delta G(1,2)}{\delta U(3,4)}=-G_2(1,4;2,3)+G(1,2)G(4,3). \tag{18.12}$$

Using this relation in Equation 18.11, one can get

$$\int d3\left[i\delta(1,3)\frac{\partial}{\partial t_1}-h(1,3)\right]G(3,2)-\int d3\Sigma_{Hxc}(1,3)G(3,2)=\delta(1,2), \tag{18.13}$$

where $\Sigma_{Hxc}$ (1,2) is the Hartree exchange-correlation self-energy that takes into account all the two-particle effects. It can be decomposed into a Hartree contribution

$$\Sigma_H(1,2)=-i\int d3d3'v(1,3;2,3')G(3'^{+},3^{++}), \tag{18.14}$$

and an exchange-correlation one

$$\Sigma_{xc}(1,2)=i\int d3d1'd3'd4v(1,3;1',3')\frac{\delta G(1',4)}{\delta U(3^{++},3'^{+})}G^{-1}(4,2). \tag{18.15}$$

One can define a Green's function $G_h$ which shows no two-particle effects and therefore follows the equation of motion:

$$\int d3\left[i\delta(1,3)\frac{\partial}{\partial t_1}-h(1,3)\right]G_h(3,2)=\delta(1,2). \tag{18.16}$$

Using this relation in Equation 18.13, one finally gets the Dyson equation for the one-particle Green's function:

$$\int d3\left[G_h^{-1}(1,3)-\Sigma_{Hxc}(1,3)\right]G(3,2)=\delta(1,2). \tag{18.17}$$

This equation is also often used under the form

$$G(1,2)=G_h(1,2)+\int d3d4G_h(1,3)\Sigma_{Hxc}(3,4)G(4,2), \tag{18.18}$$

or

$$G^{-1}(1,2)=G_h^{-1}(1,2)-\Sigma_{Hxc}(1,2). \tag{18.19}$$

### 18.2.4 Bethe–Salpeter Equation

Starting from the Dyson equation (see Equation 18.19), and taking the derivative with respect to $G$, one can get the so-called BSE (see, e.g., reference [35]):

$$\chi^{-1}(1,2;1',2')=\chi_{IP}^{-1}(1,2;1',2')-\Xi_{Hxc}(1,2;1',2'), \tag{18.20}$$

or

$$\chi(1,2;1',2')=\chi_{IP}(1,2;1',2')+\int d3d4d5d6\chi_{IP}(1,4;1',3)\Xi_{Hxc}(3,6;4,5)\chi(5,2;6,2'), \tag{18.21}$$

where $\Xi_{Hxc}$ is the Hartree-exchange-correlation Bethe–Salpeter kernel defined as

$$\Xi_{Hxc}(3,6;4,5)=i\frac{\delta\Sigma_{Hxc}(3,4)}{\delta G(5,6)}. \tag{18.22}$$

### 18.2.5 Hedin's Equations

We now have equations of motion for the one- and two-particle Green's functions. They depend on the Hartree-exchange-correlation self-energy. Its Hartree part is trivial, but a practical way of calculating its exchange-correlation part is needed. Hedin [36] proposed a scheme that yields to a set of coupled equations and allows in principle for the calculation of the exact self-energy. This scheme can be seen as a perturbation theory in terms of the screened interaction $W$ instead of the bare Coulomb interaction $v$. We show a generalization of this derivation for the case of a nonlocal potential.

Let $V(5,6) = U(5,6) - i\int d3d3' v(5,3;6,3')G(3',3^+)$ be the nonlocal classic potential. Using the chain rule in the exchange-correlation self-energy, we get

$$\begin{aligned}\Sigma_{xc}(1,2) &= -i\int d3d1'd3'd4d5d6 v(1,3;1',3')G(1',4)\frac{\delta G^{-1}(4,2)}{\delta V(5,6)}\frac{\delta V(5,6)}{\delta U(3^{++},3'^{+})} \\ &= i\int d3d1'd3'd4d5d6 v(1,3;1',3')G(1',4)\tilde{\Gamma}(4,6;2,5)\epsilon^{-1}(5,3';6,3^+),\end{aligned} \tag{18.23}$$

where the inverse dielectric function $\epsilon^{-1}$ that screens the bare Coulomb interaction $v$ and the irreducible vertex function $\tilde{\Gamma}$ are defined by

$$\epsilon^{-1}(1,2;3,4) = \frac{\delta V(1,3)}{\delta U(4,2)} \text{ and } \tilde{\Gamma}(1,2;3,4) = -\frac{\delta G^{-1}(1,3)}{\delta V(4,2)}. \tag{18.24}$$

We can therefore define a dynamically screened potential

$$\begin{aligned}W(1,2;1',2') &= \int d3d3'\epsilon^{-1}(1,3;1',3'^{+})v(2,3';2',3) \\ &= \int d3d3'\epsilon^{-1}(1,3;1',3'^{+})v(3',2;3,2'),\end{aligned} \tag{18.25}$$

where the symmetry of the Coulomb interaction $v$ has been used, and we get the expression of the exchange-correlation self-energy:

$$\Sigma_{xc}(1,2) = i\int d1'd3d3'd4 G(1',4)\tilde{\Gamma}(4,3',2,3)W(3,1;3',1'). \tag{18.26}$$

We still need to express the dielectric function and the irreducible vertex function without the use of $V$ and $U$. To achieve this, we define the irreducible polarizability $\tilde{\chi}(1,2;3,4) = -i\delta G(1,3)/\delta V(4,2)$, which, with the properties of the inverse and the definition of the vertex correction, can be rewritten as

$$\tilde{\chi}(1,2;3,4) = -i\int d5d5' G(1,5)G(5',3)\tilde{\Gamma}(5,2;5',4). \tag{18.27}$$

Using this relation, one can rewrite the dielectric function as

$$\epsilon(1,2;3,4) = \delta(1,4)\delta(2,3) - \int d5d5' v(1,5;3,5')\tilde{\chi}(5',2;5^+,4), \tag{18.28}$$

and the irreducible vertex correction as

$$\tilde{\Gamma}(1,2;3,4) = \delta(1,4)\delta(2,3) - i\int d5d6 \frac{\delta\Sigma_{xc}(1,3)}{\delta G(5,6)}\tilde{\chi}(5,2;6,4). \tag{18.29}$$

We now have a set of five coupled equations (see Equations 18.25 through 18.29) to calculate the self-energy. In practice, this set of equations is never solved exactly, and approximations are made.

### 18.2.6 Static GW Approximation

We discuss now the static GW approximation that is the most often used approximation in practice in the BSE approach.

In the GW approximation, one takes $\tilde{\Gamma}(1,2;3,4) = \delta(1,4)\delta(2,3)$. This greatly simplifies Hedin's equations. The irreducible polarizability becomes $\tilde{\chi}(1,2;3,4) = -iG(1,4)G(2,3) = \chi_{IP}(1,2;3,4)$, and the exchange-correlation self-energy becomes

$$\Sigma_{xc}(1,2) = i\int d1'd3G(1',3)W(3,1;2,1'). \tag{18.30}$$

If the derivative of $W$ with respect to $G$ is further neglected, as usually done, the corresponding Bethe–Salpeter kernel is then

$$\Xi_{Hxc}(1,2;1',2') = v(1,2;1',2') - W(2,1;1',2'). \tag{18.31}$$

where $W$ is obtained from Equation 18.25 and $\epsilon^{-1}$ with Equation 18.28 in which $\tilde{\chi}$ is replaced by $\chi_{IP}$. The Coulomb interaction is instantaneous, and the one-particle Green's function depends only on the time difference; therefore, the time dependence of the screened interaction is

$$W(1,2;1',2') = W(\mathbf{x}_1,\mathbf{x}_2;\mathbf{x}_1',\mathbf{x}_2';\tau)\delta(t_1,t_1')\delta(t_2,t_2'), \tag{18.32}$$

where $\tau = t_1 - t_2$. If one considers the time dependence in $W$, the Fourier transform of the BSE is not straightforward.[32] We will only consider the usual approximation where the screened interaction is static, that is,

$$W(1,2;1',2') = W(\mathbf{x}_1,\mathbf{x}_2;\mathbf{x}_1',\mathbf{x}_2')\delta(t_1,t_1')\delta(t_2,t_2')\delta(t_1,t_2). \tag{18.33}$$

To summarize, the Fourier-space BSE in the static GW approximation writes

$$\chi^{-1}(\mathbf{x}_1,\mathbf{x}_2;\mathbf{x}_3,\mathbf{x}_4;\omega) = \chi_{IP}^{-1}(\mathbf{x}_1,\mathbf{x}_2;\mathbf{x}_3,\mathbf{x}_4;\omega) - \Xi_{Hxc}(\mathbf{x}_1,\mathbf{x}_2;\mathbf{x}_3,\mathbf{x}_4), \tag{18.34}$$

where the kernel $\Xi_{Hxc}(\mathbf{x}_1,\mathbf{x}_2;\mathbf{x}_3,\mathbf{x}_4) = v(\mathbf{x}_1,\mathbf{x}_2;\mathbf{x}_3,\mathbf{x}_4) - W(\mathbf{x}_2,\mathbf{x}_1;\mathbf{x}_3,\mathbf{x}_4)$ contains the static screened interaction $W$ calculated from

$$W(\mathbf{x}_1,\mathbf{x}_2;\mathbf{x}_1',\mathbf{x}_2') = \int d\mathbf{x}_3\, d\mathbf{x}_3'\epsilon^{-1}(\mathbf{x}_1,\mathbf{x}_3;\mathbf{x}_1',\mathbf{x}_3')v(\mathbf{x}_3',\mathbf{x}_2;\mathbf{x}_3,\mathbf{x}_2'), \tag{18.35}$$

and

$$\epsilon(\mathbf{x}_1,\mathbf{x}_2;\mathbf{x}_3,\mathbf{x}_4)=\delta(\mathbf{x}_1,\mathbf{x}_4)\delta(\mathbf{x}_2,\mathbf{x}_3)-\int d\mathbf{x}_5\, d\mathbf{x}'_5 v(\mathbf{x}_1,\mathbf{x}_5;\mathbf{x}_3,\mathbf{x}'_5)\chi_{IP}(\mathbf{x}'_5,\mathbf{x}_2;\mathbf{x}_5,\mathbf{x}_4;\omega=0). \tag{18.36}$$

We will refer to the approach of Equations 18.34 through 18.36 as the BSE-GW method. The one-particle Green's function $G$ in $\chi_{IP} = -iGG$ is not yet specified. Different choices can be made. The simplest option is to use a noninteracting Green's function $G_0$ from a Hartree–Fock (HF) or Kohn–Sham (KS) calculation. In this case, $\chi_{IP} = -iG_0G_0 = \chi_0$ is just the noninteracting HF or KS response function. In the condensed-matter physics literature, the usual recipe is to use $\chi_0$ in Equation 18.36 but an improved $\chi_{IP}$ in Equation 18.34 from a GW calculation. In the case of $H_2$ in a minimal basis, it is simple enough to use $\chi_{IP}$ constructed with the exact one-particle Green's function $G$. Finally, we note that the dielectric function of Equation 18.36 could be alternatively defined as including the HF exchange in addition to the Coulomb interaction, that is, $v(\mathbf{x}_1,\mathbf{x}_5;\mathbf{x}_3,\mathbf{x}'_5) \to v(\mathbf{x}_1,\mathbf{x}_5;\mathbf{x}_3,\mathbf{x}'_5) - v(\mathbf{x}_5,\mathbf{x}_1;\mathbf{x}_3,\mathbf{x}'_5)$ (see, e.g., reference [37]), which removes the "self-screening error" for one-electron systems,[38] but we do not explore this possibility here.

## 18.3 EXPRESSIONS IN FINITE ORBITAL BASIS

### 18.3.1 Spin-Orbital Basis

To solve the BSE for finite systems, all the equations are projected onto an orthonormal spin-orbital basis $\{\phi_p\}$. As the equations are four-point equations relating two-particle quantities, they are in fact projected onto the basis of products of two spin orbitals. Each matrix element is thus indexed by two double indices.

We consider the simplest case for which $\chi_{IP} = \chi_0$. The Lehmann representation of $\chi_0$ is

$$\chi_0(\mathbf{x}_1,\mathbf{x}_2;\mathbf{x}'_1,\mathbf{x}'_2;\omega)=\sum_{ia}\frac{\phi_i^*(\mathbf{x}'_1)\phi_a(\mathbf{x}_1)\phi_a^*(\mathbf{x}'_2)\phi_i(\mathbf{x}_2)}{\omega-(\varepsilon_a-\varepsilon_i)+i0^+}-\frac{\phi_i^*(\mathbf{x}'_2)\phi_a(\mathbf{x}_2)\phi_a^*(\mathbf{x}'_1)\phi_i(\mathbf{x}_1)}{\omega+(\varepsilon_a-\varepsilon_i)-i0^+}, \tag{18.37}$$

where $\phi_i$ is the $i$th occupied spin orbital of energy $\varepsilon_i$, and $\phi_a$ is the $a$th virtual spin orbital of energy $\varepsilon_a$. One can notice that $\chi_0$ is expanded only on occupied-virtual (ov) and virtual-occupied (vo) products of spin orbitals. The matrix elements of $\chi_0$ are given by

$$\left[\chi_0(\omega)\right]_{pq,rs}=\int d\mathbf{x}_1\, d\mathbf{x}'_1\, d\mathbf{x}_2\, d\mathbf{x}'_2\phi_p(\mathbf{x}'_1)\phi_q^*(\mathbf{x}_1)\chi_0(\mathbf{x}_1,\mathbf{x}_2;\mathbf{x}'_1,\mathbf{x}'_2;\omega)\phi_r^*(\mathbf{x}_2)\phi_s(\mathbf{x}'_2). \tag{18.38}$$

The matrix representation of its inverse, in the (ov,vo) subspace, is

$$\boldsymbol{\chi}_0^{-1}(\omega)=-\left[\begin{pmatrix}\Delta\boldsymbol{\varepsilon} & \mathbf{0}\\ \mathbf{0} & \Delta\boldsymbol{\varepsilon}\end{pmatrix}-\omega\begin{pmatrix}\mathbf{1} & \mathbf{0}\\ \mathbf{0} & -\mathbf{1}\end{pmatrix}\right], \tag{18.39}$$

where $\Delta\varepsilon_{ia,jb} = \Delta\varepsilon_{ai,bj} = (\varepsilon_a - \varepsilon_i)\delta_{ij}\delta_{ab}$, where $i,j$ refers to occupied spin orbitals, and $a,b$ refers to virtual spin orbitals. The dimension of the matrix is thus $2M_oM_v \times 2M_oM_v$, where $M_o$ and $M_v$ are the numbers of occupied and virtual spin orbitals, respectively. To build the matrix $\boldsymbol{\chi}^{-1}$, one then needs to construct the matrix elements of the Bethe–Salpeter kernel $\Xi_{Hxc}$, which are given by

$$(\Xi_{Hxc})_{pq,rs} = \mathrm{v}_{pq,rs} - W_{pr,qs}, \tag{18.40}$$

where $v_{pq,rs} = \langle qr|ps\rangle$ are the usual two-electron integrals, and the matrix elements of $W$ can be obtained from Equation 18.35:

$$\begin{aligned} W_{pq,rs} &= \int d\mathbf{x}_1\, d\mathbf{x}_1'\, d\mathbf{x}_2\, d\mathbf{x}_2' \phi_p(\mathbf{x}_1')\phi_q^*(\mathbf{x}_1) \\ &\quad \times W(\mathbf{x}_1,\mathbf{x}_2;\mathbf{x}_1',\mathbf{x}_2')\phi_r^*(\mathbf{x}_2)\phi_s(\mathbf{x}_2') \\ &= \int d\mathbf{x}_1\, d\mathbf{x}_1'\, d\mathbf{x}_2\, d\mathbf{x}_2'\, d\mathbf{x}_3\, d\mathbf{x}_3' \phi_p(\mathbf{x}_1')\phi_q^*(\mathbf{x}_1) \\ &\quad \times \epsilon^{-1}(\mathbf{x}_1,\mathbf{x}_3;\mathbf{x}_1',\mathbf{x}_3')v(\mathbf{x}_3',\mathbf{x}_2;\mathbf{x}_3,\mathbf{x}_2')\phi_r^*(\mathbf{x}_2)\phi_s(\mathbf{x}_2'). \end{aligned} \tag{18.41}$$

To decouple the common coordinates in $\epsilon^{-1}$ and $v$, one can introduce two delta functions $\delta(\mathbf{x}_3,\mathbf{x}_4)$ and $\delta(\mathbf{x}_3',\mathbf{x}_4')$ and use the closure relations $\delta(\mathbf{x}_3,\mathbf{x}_4) = \sum_t \phi_t^*(\mathbf{x}_3)\phi_t(\mathbf{x}_4)$ and $\delta(\mathbf{x}_3',\mathbf{x}_4') = \sum_u \phi_u(\mathbf{x}_3')\phi_u^*(\mathbf{x}_4')$. By doing so, the matrix elements of $v$ and $\epsilon^{-1}$ appear explicitly, and we get

$$W_{pq,rs} = \sum_{tu} \epsilon^{-1}_{pq,tu} v_{tu,rs}. \tag{18.42}$$

Similarly, for the dielectric function, we have

$$\epsilon_{pq,rs} = \delta_{pr}\delta_{qs} - \sum_{tu} v_{pq,tu}\left[\chi_0(\omega=0)\right]_{tu,rs} = \delta_{pr}\delta_{qs} - v_{pq,rs}\left[\chi_0(\omega=0)\right]_{rs,rs}, \tag{18.43}$$

where the last equality comes from the fact that $\chi_0$ has only diagonal elements. It can be seen that the static screened interaction consists of an infinite-order perturbation expansion in the Coulomb interaction, namely, using matrix notations,

$$\boldsymbol{W} = \boldsymbol{\epsilon}^{-1}\cdot\boldsymbol{v} = \boldsymbol{v} + \boldsymbol{v}\cdot\boldsymbol{\chi}_0(\omega=0)\cdot\boldsymbol{v} + \boldsymbol{v}\cdot\boldsymbol{\chi}_0(\omega=0)\cdot\boldsymbol{v}\cdot\boldsymbol{\chi}_0(\omega=0)\cdot\boldsymbol{v} + \ldots, \tag{18.44}$$

with the first term in this expansion corresponding to time-dependent HF (TDHF). The matrix representation of the inverse of the interacting response function, in the (ov,vo) subspace, is then

$$\boldsymbol{\chi}^{-1}(\omega) = -\left[\begin{pmatrix} \boldsymbol{A} & \boldsymbol{B} \\ \boldsymbol{B}^* & \boldsymbol{A}^* \end{pmatrix} - \omega\begin{pmatrix} \mathbf{1} & \mathbf{0} \\ \mathbf{0} & -\mathbf{1} \end{pmatrix}\right], \tag{18.45}$$

with the matrices

$$A_{ia,jb} = \Delta\varepsilon_{ia,jb} + v_{ia,jb} - W_{ij,ab}, \tag{18.46}$$

$$B_{ia,jb} = v_{ia,bj} - W_{ib,aj}. \tag{18.47}$$

The block structure of Equation 18.45 is a consequence of the symmetry of the Coulomb interaction, $v_{qp,sr} = v^*_{pq,rs}$, and the static screened interaction, $W_{qs,pr} = W^*_{pr,qs}$. Moreover, the matrix $\boldsymbol{A}$ is Hermitian (because $v_{ia,jb} = v^*_{jb,ia}$ and $W_{ij,ab} = W^*_{ji,ba}$), and the matrix $\boldsymbol{B}$ is symmetric (because $v_{ia,bj} = v_{jb,ai}$ and $W_{ib,aj} = W_{ja,bi}$). The excitation energies $\omega_n$ are thus found by solving the usual linear response pseudo-Hermitian eigenvalue equation, just as in TDDFT,

$$\begin{pmatrix} \boldsymbol{A} & \boldsymbol{B} \\ \boldsymbol{B}^* & \boldsymbol{A}^* \end{pmatrix} \begin{pmatrix} \boldsymbol{X}_n \\ \boldsymbol{Y}_n \end{pmatrix} = \omega_n \begin{pmatrix} \mathbf{1} & \mathbf{0} \\ \mathbf{0} & -\mathbf{1} \end{pmatrix} \begin{pmatrix} \boldsymbol{X}_n \\ \boldsymbol{Y}_n \end{pmatrix}, \tag{18.48}$$

whose solutions come in pairs: excitation energies $\omega_n$ with eigenvectors $(\boldsymbol{X}_n, \boldsymbol{Y}_n)$ and deexcitation energies $-\omega_n$ with eigenvectors $\left(\boldsymbol{Y}^*_n, \boldsymbol{X}^*_n\right)$. For real spin orbitals and if $\boldsymbol{A} + \boldsymbol{B}$ and $\boldsymbol{A} - \boldsymbol{B}$ are positive definite, the eigenvalues are guaranteed to be real numbers, and the pseudo-Hermitian eigenvalue equation (see Equation 18.48) can be transformed into a half-size symmetric eigenvalue equation (see Equation 18.3).

If, instead of starting from $\chi_0$, one starts from $\chi_{IP} = -iGG$ with the exact one-particle Green's function $G$, the equations get more complicated because the matrix representation of $\chi_{IP}$ is generally not diagonal and has contributions not only in the (ov,vo) subspace of spin-orbital products but also in the occupied–occupied (oo) and virtual–virtual (vv) subspace of spin-orbital products. The dimension of the matrices thus becomes $M^2 \times M^2$, where $M$ is the total number of (occupied and virtual) spin orbitals. In this case, the number of solutions of the response equations is generally higher than the number of single excitations, and in particular, double excitations might be obtained even without a frequency-dependent kernel. Spurious excitations are also found. This is similar to what happens in linear response TDDMFT.[12–15] We will show this later in the case of $H_2$ in a minimal basis.

### 18.3.2 Spin Adaptation

We give now the expressions for spin-restricted closed-shell calculations. For four fixed spatial orbitals referred to as $p$, $q$, $r$, and $s$, the Bethe–Salpeter kernel has the following spin structure:

$$\begin{pmatrix} \Xi_{p\uparrow q\uparrow,r\uparrow s\uparrow} & \Xi_{p\uparrow q\uparrow,r\downarrow s\downarrow} & 0 & 0 \\ \Xi_{p\downarrow q\downarrow,r\uparrow s\uparrow} & \Xi_{p\downarrow q\downarrow,r\downarrow s\downarrow} & 0 & 0 \\ 0 & 0 & \Xi_{p\uparrow q\downarrow,r\uparrow s\downarrow} & \Xi_{p\uparrow q\downarrow,r\downarrow s\uparrow} \\ 0 & 0 & \Xi_{p\downarrow q\uparrow,r\uparrow s\downarrow} & \Xi_{p\downarrow q\uparrow,r\downarrow s\uparrow} \end{pmatrix}, \tag{18.49}$$

which can be brought to a diagonal form after rotation (see, e.g., refs. [35], [39], and [40]):

$$\begin{pmatrix} {}^1\Xi_{pq,rs} & 0 & 0 & 0 \\ 0 & {}^3\Xi_{pq,rs} & 0 & 0 \\ 0 & 0 & {}^3\Xi_{pq,rs} & 0 \\ 0 & 0 & 0 & {}^3\Xi_{pq,rs} \end{pmatrix}, \tag{18.50}$$

with a spin-singlet term ${}^1\Xi_{pq,rs} = 2v_{pq,rs} - W_{pr,qs}$ and three degenerate spin-triplet terms ${}^3\Xi_{pq,rs} = -W_{pr,qs}$. It has been used that the Coulomb interaction $v$ and the screened interaction $W$ are spin independent: $v_{pq,rs} = v_{p\uparrow q\uparrow,r\uparrow s\uparrow} = v_{p\uparrow q\uparrow,r\downarrow s\downarrow} = v_{p\downarrow q\downarrow,r\uparrow s\uparrow} = v_{p\downarrow q\downarrow,r\downarrow s\downarrow}$ and $W_{pq,rs} = W_{p\uparrow q\uparrow,r\uparrow s\uparrow} = W_{p\uparrow q\uparrow,r\downarrow s\downarrow} = W_{p\downarrow q\downarrow,r\uparrow s\uparrow} = W_{p\downarrow q\downarrow,r\downarrow s\downarrow}$. The spin-adapted screened interaction is obtained by

$$W_{pq,rs} = \sum_{tu} {}^1\epsilon^{-1}_{pq,tu} v_{tu,rs}, \tag{18.51}$$

where $t$ and $u$ refer to spatial orbitals, and the singlet dielectric function ${}^1\epsilon_{pq,rs} = \epsilon_{p\uparrow q\uparrow,r\uparrow s\uparrow} + \epsilon_{p\uparrow q\uparrow,r\downarrow s\downarrow}$ is given by

$${}^1\epsilon_{pq,rs} = \delta_{pr}\delta_{qs} - 2v_{pq,rs}\left[\chi_0(\omega = 0)\right]_{rs,rs}. \tag{18.52}$$

The bottom line is that the linear response eigenvalue equation (see Equation 18.48) decouples into a singlet eigenvalue equation

$$\begin{pmatrix} {}^1\boldsymbol{A} & {}^1\boldsymbol{B} \\ {}^1\boldsymbol{B}^* & {}^1\boldsymbol{A}^* \end{pmatrix} \begin{pmatrix} {}^1\boldsymbol{X}_n \\ {}^1\boldsymbol{Y}_n \end{pmatrix} = {}^1\omega_n \begin{pmatrix} \mathbf{1} & \mathbf{0} \\ \mathbf{0} & -\mathbf{1} \end{pmatrix} \begin{pmatrix} {}^1\boldsymbol{X}_n \\ {}^1\boldsymbol{Y}_n \end{pmatrix}, \tag{18.53}$$

with the matrices

$${}^1A_{ia,jb} = \Delta\varepsilon_{ia,jb} + 2v_{ia,jb} - W_{ij,ab}, \tag{18.54}$$

$${}^1B_{ia,jb} = 2v_{ia,bj} - W_{ib,aj}, \tag{18.55}$$

and a triplet eigenvalue equation

$$\begin{pmatrix} {}^3\boldsymbol{A} & {}^3\boldsymbol{B} \\ {}^3\boldsymbol{B}^* & {}^3\boldsymbol{A}^* \end{pmatrix} \begin{pmatrix} {}^3\boldsymbol{X}_n \\ {}^3\boldsymbol{Y}_n \end{pmatrix} = {}^3\omega_n \begin{pmatrix} \mathbf{1} & \mathbf{0} \\ \mathbf{0} & -\mathbf{1} \end{pmatrix} \begin{pmatrix} {}^3\boldsymbol{X}_n \\ {}^3\boldsymbol{Y}_n \end{pmatrix}, \tag{18.56}$$

with the matrices

$$^3A_{ia,jb} = \Delta\varepsilon_{ia,jb} - W_{ij,ab}, \tag{18.57}$$

$$^3B_{ia,jb} = -W_{ib,aj}. \tag{18.58}$$

## 18.4 EXAMPLE OF $H_2$ IN A MINIMAL BASIS

As a pedagogical example, we apply the BSE-GW method to the calculation of the excitation energies of $H_2$ in a minimal basis consisting of two Slater basis functions, $\varphi_a$ and $\varphi_b$, centered on each hydrogen atom and with the same exponent $\zeta = 1$. This is a closed-shell molecule; therefore, all the calculations are done with spin adaptation in a spatial orbital basis. The molecular orbitals are $\psi_1 = (\ _a + \ _b)/\sqrt{2(1+S_{ab})}$ (symmetry $\sigma_g$) and $\psi_2 = (\ _a - \ _b)/\sqrt{2(1-S_{ab})}$ (symmetry $\sigma_u$), where $S_{ab}$ is the overlap between $\varphi_a$ and $\varphi_b$. The matrix representations of all two-electron quantities in the space of spatial–orbital products are of the following form:

$$\boldsymbol{P} = \left(\begin{array}{cc|cc} P_{11,11} & P_{11,22} & P_{11,12} & P_{11,21} \\ P_{22,11} & P_{22,22} & P_{22,12} & P_{22,21} \\ \hline P_{12,11} & P_{12,22} & P_{12,12} & P_{12,21} \\ P_{21,11} & P_{21,22} & P_{21,12} & P_{21,21} \end{array}\right), \tag{18.59}$$

and we refer to the upper left block as the (oo,vv) block and to the bottom right block as the (ov,vo) block. All the values of the integrals as a function of the internuclear distance $R$ can be found in reference [41]. Note that, in the condensed-matter physics literature, a simplified version of $H_2$ in a minimal basis with only on-site Coulomb interaction is often used under the name "half-filled two-site Hubbard model" (see, e.g., references [38] and [42])*.

### 18.4.1 BSE-GW Method Using the Noninteracting Green's Function

The simplest approximation in the BSE-GW method is to start from the noninteracting HF Green's function $G_0$, leading to the noninteracting HF linear response function $\chi_{IP} = -iG_0G_0 = \chi_0$ whose matrix representation reads

$$\boldsymbol{\chi}_0(\omega) = \left(\begin{array}{cc|cc} 0 & 0 & 0 & 0 \\ 0 & 0 & 0 & 0 \\ \hline 0 & 0 & \dfrac{1}{\omega - \Delta\varepsilon} & 0 \\ 0 & 0 & 0 & \dfrac{-1}{\omega + \Delta\varepsilon} \end{array}\right), \tag{18.60}$$

* With the notations used here, the Hubbard model is obtained for $\Delta\varepsilon = 2t$ and $J_{11} = J_{22} = J_{12} = K_{12} = U/2$ where $t$ is the hopping parameter and $U$ is the on-site Coulomb interaction.

where $\Delta\varepsilon = \varepsilon_2 - \varepsilon_1$ is the difference between the energies of the molecular orbitals $\psi_2$ and $\psi_1$. The noninteracting linear response function has nonvanishing matrix elements only in the (ov,vo) block, but it will be necessary to consider the other blocks as well for the screened interaction *W*. The matrix of the Coulomb interaction is

$$\mathbf{v} = \left(\begin{array}{cc|cc} J_{11} & J_{12} & 0 & 0 \\ J_{12} & J_{22} & 0 & 0 \\ \hline 0 & 0 & K_{12} & K_{12} \\ 0 & 0 & K_{12} & K_{12} \end{array}\right), \tag{18.61}$$

where $J_{pq} = \langle pq|pq\rangle$ and $K_{pq} = \langle pq|qp\rangle$ are the usual Coulomb and exchange two-electron integrals over the molecular orbitals $\psi_1$ and $\psi_2$. The off-diagonal blocks of *v* are zero by symmetry for $H_2$ in a minimal basis, but this is not the case in general. By matrix product and inversion, we get the static singlet dielectric matrix

$${}^1\boldsymbol{\epsilon} = \left(\begin{array}{cc|cc} 1 & 0 & 0 & 0 \\ 0 & 1 & 0 & 0 \\ \hline 0 & 0 & 1+\dfrac{2K_{12}}{\Delta\varepsilon} & \dfrac{2K_{12}}{\Delta\varepsilon} \\ 0 & 0 & \dfrac{2K_{12}}{\Delta\varepsilon} & 1+\dfrac{2K_{12}}{\Delta\varepsilon} \end{array}\right), \tag{18.62}$$

which, in this case, is block diagonal with the (oo,vv) block being the identity. By using its inverse, we finally get the static screened interaction matrix

$$\mathbf{W} = \left(\begin{array}{cc|cc} J_{11} & J_{12} & 0 & 0 \\ J_{12} & J_{22} & 0 & 0 \\ \hline 0 & 0 & \dfrac{K_{12}}{1+4K_{12}/\Delta\varepsilon} & \dfrac{K_{12}}{1+4K_{12}/\Delta\varepsilon} \\ 0 & 0 & \dfrac{K_{12}}{1+4K_{12}/\Delta\varepsilon} & \dfrac{K_{12}}{1+4K_{12}/\Delta\varepsilon} \end{array}\right), \tag{18.63}$$

which is block diagonal and the (oo,vv) block is just the bare Coulomb interaction in the case of $H_2$ in a minimal basis, but this is not generally true. We have then everything to construct the ${}^1A$ and ${}^1B$ matrices of Equation 18.53 for singlet excitations, which in the present case are just one-dimensional

$${}^1A = \Delta\varepsilon + 2K_{12} - J_{12}, \tag{18.64}$$

and

$${}^1B = 2K_{12} - \frac{K_{12}}{1+4K_{12}/\Delta\varepsilon}, \tag{18.65}$$

and the $^3A$ and $^3B$ matrices of Equation 18.56 for triplet excitations

$$^3A = \Delta\varepsilon - J_{12}, \tag{18.66}$$

and

$$^3B = -\frac{K_{12}}{1+4K_{12}/\Delta\varepsilon}. \tag{18.67}$$

Solving then the response equations by the standard Casida approach,[3] we get the singlet excitation energy

$$^1\omega = \sqrt{\left(\Delta\varepsilon + 4K_{12} - J_{12} - \frac{K_{12}}{1+4K_{12}/\Delta\varepsilon}\right)\left(\Delta\varepsilon - J_{12} + \frac{K_{12}}{1+4K_{12}/\Delta\varepsilon}\right)}, \tag{18.68}$$

and the triplet excitation energy

$$^3\omega = \sqrt{\left(\Delta\varepsilon - J_{12} - \frac{K_{12}}{1+4K_{12}/\Delta\varepsilon}\right)\left(\Delta\varepsilon - J_{12} + \frac{K_{12}}{1+4K_{12}/\Delta\varepsilon}\right)}. \tag{18.69}$$

Note that, for this simple system, the $A$ terms have the usual TDHF or configuration interaction single (CIS) forms, and the screening has an effect only on the $B$ terms, decreasing the exchange integral $K_{12}$ by a factor of $1 + 4K_{12}/\Delta\varepsilon$. Therefore, in the Tamm–Dancoff approximation,[43] which consists of neglecting $B$, the effect of screening would be lost and the method would be equivalent to CIS. It is interesting to analyze the effect of the screening as a function of the internuclear distance $R$. For small $R$, the orbital energy difference $\Delta\varepsilon$ is much greater than the exchange integral $K_{12}$, so the screening factor $1 + 4K_{12}/\Delta\varepsilon$ is close to 1 and TDHF excitation energies are recovered. For large $R$ (dissociation limit), $\Delta\varepsilon$ goes to zero, so the screening factor diverges and the term $K_{12}/(1 + 4K_{12}/\Delta\varepsilon)$ vanishes.

The excitation energies from the ground state $^1\Sigma_g^+$ to the first singlet $^1\Sigma_u^+$ and triplet $^3\Sigma_u^+$ excited states are plotted as a function of $R$ in Figure 18.1. The reference curves are from a full configuration-interaction (FCI) calculation giving the exact excitation energies on this basis. In a minimal basis, the singlet $^1\Sigma_u^+$ excited state is constrained to dissociate into the ionic configuration $H^-\ldots H^+$; so in the dissociation limit $R \to \infty$, the exact singlet excitation energy goes to a constant, $I - A \approx 0.625$ hartree, where $I$ and $A$ are the ionization energy and electron affinity of the hydrogen atom, respectively. The triplet $^3\Sigma_u^+$ dissociates into the neutral configuration $H^\bullet\ldots H^\bullet$, as does the ground state, so the exact triplet excitation energy goes to zero in the dissociation limit. TDHF gives accurate excitation energies for small $R$ but gives qualitatively wrong curves in the dissociation limit. For the singlet state, the TDHF excitation energy goes to zero, a wrong behavior inherited from the vanishing

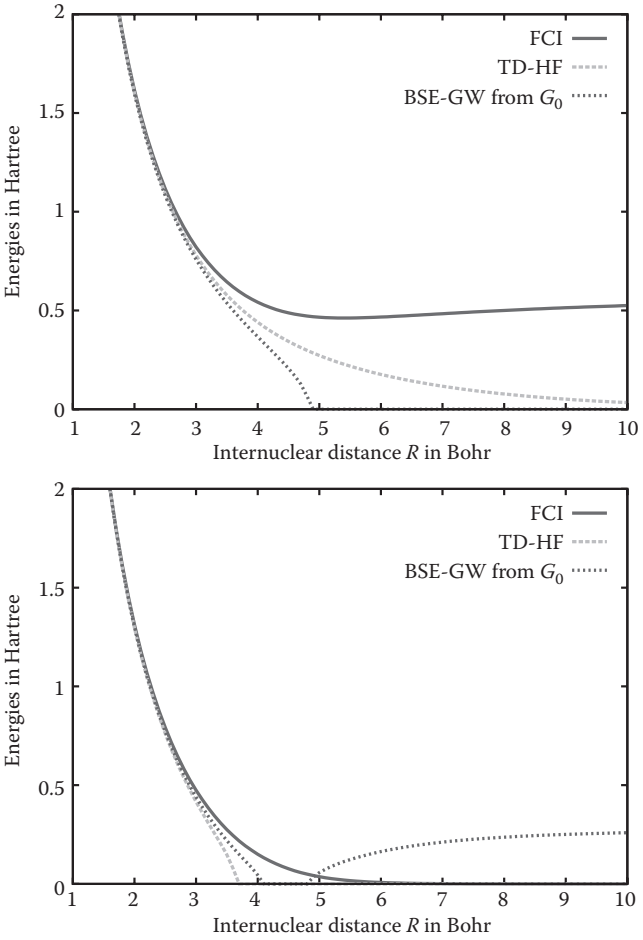


**FIGURE 18.1** Excitation energies of the singlet ${}^1\Sigma_u^+$ (top) and triplet ${}^3\Sigma_u^+$ (bottom) states of $H_2$ in a minimal basis as a function of the internuclear distance $R$ calculated by FCI, TDHF, and BSE-GW with the noninteracting HF Green's function $G_0$.

$\Delta\varepsilon$ in this limit. For the triplet state, the TDHF response equation suffers from a triplet instability for $R \geq 4$ Bohr and the excitation energy becomes imaginary. It is known that TDDFT with standard density functional approximations gives similarly incorrect energy curves.[7,42,44–46] The BSE-GW method using the noninteracting HF Green's function $G_0$ gives accurate excitation energies at small $R$ but fails in the dissociation limit. The singlet excitation energy becomes imaginary for $R \geq 4.9$ Bohr. Indeed, in the dissociation limit, $\Delta\varepsilon$ goes to zero and Equation 18.68 leads to a negative term under the square root: ${}^1\omega \rightarrow \sqrt{(4K_{12} - J_{12})(-J_{12})}$. Similarly, the BSE-GW triplet excitation energy is imaginary between $R = 4.0$ and $R = 4.9$ Bohr and incorrectly tends to a nonzero value in the dissociation limit.

The BSE-GW method using the noninteracting HF Green's function $G_0$ thus badly fails for $H_2$ in the dissociation limit. As this method is based on a single-determinant reference, this should not come as a surprise. However, the BSE approach also allows one to start from an interacting Green's function $G$, taking into account the multiconfigurational character of stretched $H_2$. We will now test this alternative approach.

## 18.4.2 BSE-GW Method Using the Exact Green's Function

### 18.4.2.1 Independent-Particle Response Function

We apply the BSE-GW equations (see Equations 18.34 through 18.36) with the IP response function $\chi_{IP} = -iGG$ constructed from the exact one-particle Green's function $G$, which can be calculated by the Lehmann formula 18.8 using the $N$-electron ground state and the $(N \pm 1)$-electron states. The states to consider for $H_2$ in a minimal basis are given in Figure 18.2. The ground state is composed of two Slater determinants, and its energy is $E_N = 2\varepsilon_1 - J_{11} + E_c$, where $E_c = \Delta - \sqrt{\Delta^2 + K_{12}^2}$ is the correlation energy with $2\Delta = 2\Delta\varepsilon + J_{11} + J_{22} - 4J_{12} + 2K_{12}$. The coefficients of the determinants are determined by $c_2 = c_1 K_{12}/(\Delta + \sqrt{K_{12}^2 + \Delta^2})$ and $c_1^2 + c_2^2 = 1$. The energies of the two $(N+1)$-electron states are $E_{N+1,1} = 2\varepsilon_1 + \varepsilon_2 - J_{11}$ and $E_{N+1,2} = 2\varepsilon_2 + \varepsilon_1 - J_{11} + J_{22} - 2J_{12} + K_{12}$. The energies of the two $(N-1)$-electron states are $E_{N-1,1} = \varepsilon_1 - J_{11}$ and $E_{N-1,2} = \varepsilon_2 - 2J_{12} + K_{12}$. We thus obtain four poles for the exact one-particle Green's function. Two of them correspond to minus the electron affinities:

$$\mathcal{E}_2 = E_{N+1,1} - E_N = \varepsilon_2 - E_c, \tag{18.70}$$

$$\mathcal{E}_2' = E_{N+1,2} - E_N = 2\varepsilon_2 - \varepsilon_1 + J_{22} - 2J_{12} + K_{12} - E_c, \tag{18.71}$$

and the other two correspond to minus the ionization energies:

$$\mathcal{E}_1 = E_N - E_{N-1,1} = \varepsilon_1 + E_c, \tag{18.72}$$

$$\mathcal{E}_1' = E_N - E_{N-1,2} = 2\varepsilon_1 - \varepsilon_2 - J_{11} + 2J_{12} - K_{12} + E_c. \tag{18.73}$$

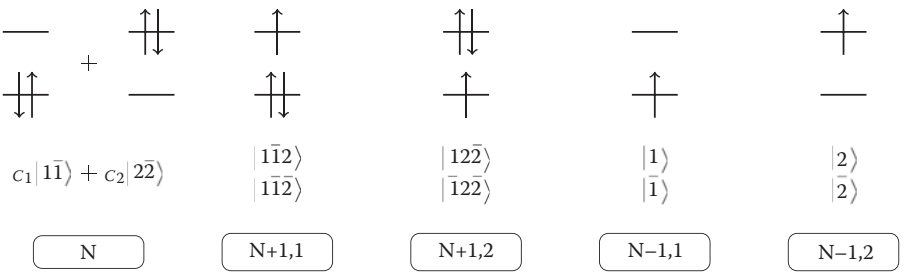


**FIGURE 18.2** $N$-electron ground state and $(N \pm 1)$-electron states for $H_2$ in a minimal basis.

In condensed-matter physics, $\mathcal{E}_1$ and $\mathcal{E}_2$ are associated with "quasi-particle" peaks of photoelectron spectra, whereas $\mathcal{E}_1'$ and $\mathcal{E}_2'$ are associated with "satellites." The Dyson orbitals are also easily calculated, and we finally arrive at the matrix representation of $\chi_{\mathrm{IP}}$ on the basis of the products of spatial orbitals

$$\boldsymbol{\chi}_{IP}(\omega) = \left(\begin{array}{cc|cc} \chi_{IP,11}(\omega) & 0 & 0 & 0 \\ 0 & \chi_{IP,22}(\omega) & 0 & 0 \\ \hline 0 & 0 & \chi_{IP,12}(\omega) & 0 \\ 0 & 0 & 0 & \chi_{IP,21}(\omega) \end{array}\right), \tag{18.74}$$

with the matrix elements

$$\chi_{IP,11}(\omega) = \frac{c_1^2 c_2^2}{\omega - (\mathcal{E}_2' - \mathcal{E}_1)} - \frac{c_1^2 c_2^2}{\omega + (\mathcal{E}_2' - \mathcal{E}_1)}, \tag{18.75}$$

$$\chi_{IP,22}(\omega) = \frac{c_1^2 c_2^2}{\omega - (\mathcal{E}_2 - \mathcal{E}_1')} - \frac{c_1^2 c_2^2}{\omega + (\mathcal{E}_2 - \mathcal{E}_1')}, \tag{18.76}$$

$$\chi_{IP,12}(\omega) = \frac{c_1^4}{\omega - (\mathcal{E}_2 - \mathcal{E}_1)} - \frac{c_2^4}{\omega + (\mathcal{E}_2' - \mathcal{E}_1')}, \tag{18.77}$$

$$\chi_{IP,21}(\omega) = \frac{c_2^4}{\omega - (\mathcal{E}_2' - \mathcal{E}_1')} - \frac{c_1^4}{\omega + (\mathcal{E}_2 - \mathcal{E}_1)}. \tag{18.78}$$

Therefore, whereas $\chi_0(\omega)$ has only one positive pole, $\chi_{\mathrm{IP}}(\omega)$ has four distinct positive poles (and four symmetric negative poles). These poles are plotted in Figure 18.3. The lowest one, $\mathcal{E}_2 - \mathcal{E}_1$, called fundamental gap in the condensed-matter physics literature, can be considered as an approximation to a neutral single excitation energy because, in the limit of noninteracting particles, it equals the difference of the orbital eigenvalues $\Delta\varepsilon = \varepsilon_2 - \varepsilon_1$. The two intermediate poles, $\mathcal{E}_2' - \mathcal{E}_1$ and $\mathcal{E}_2 - \mathcal{E}_1'$, can be interpreted as approximations to a double excitation energy because they reduce to $2\Delta\varepsilon$ in the limit of noninteracting particles. Surprisingly, the highest pole, $\mathcal{E}_2' - \mathcal{E}_1'$, reduces to $3\Delta\varepsilon$ in this limit, and it is thus tempting to associate it with a triple excitation, although the system contains only two electrons. In the dissociation limit $R \to \infty$, the four poles tend to the same value, that is, $I - A \approx 0.625$ hartree, which is also minus twice the correlation energy $-2E_c$, showing that the nonvanishing fundamental gap in this limit is a correlation effect. Note that it has been shown[38] that the non-self-consistent GW approximation ($G_0W_0$) to the one-particle Green's function gives a fundamental gap that is too small by a factor of 2 in the dissociation limit, so we do not consider this approximation here.

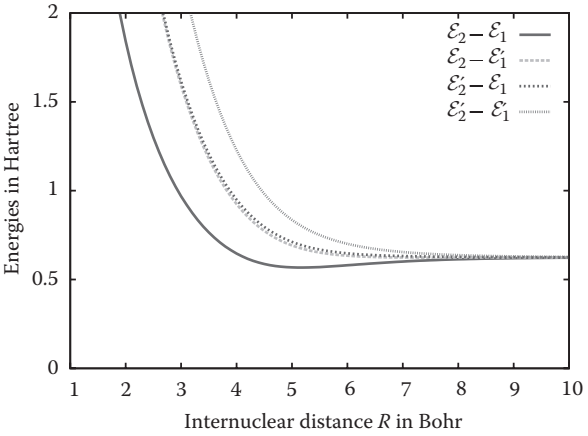


**FIGURE 18.3** Positive poles of the IP linear response function as a function of the internuclear distance $R$.

### 18.4.2.2 Excitation Energies

Having calculated the IP response function, the next steps of the BSE-GW calculation of the excitation energies continue similarly as in Section 18.4.1, although the expressions get more complicated. From the matrix $\boldsymbol{\chi}_{IP}(\omega = 0)$ and the Coulomb interaction matrix (Equation 18.61), we calculate the singlet dielectric matrix that is still block diagonal, but the upper left block is no longer the identity matrix. We calculate then the static screened interaction matrix that is still block diagonal, but the elements of its upper left block are now also affected by screening. We can then construct the corresponding singlet and triplet Bethe–Salpeter kernel ${}^1\boldsymbol{\Xi}$ and ${}^3\boldsymbol{\Xi}$. The response eigenvalue equations (see Equations 18.53 and 18.56) are no longer applicable, so the singlet excitation energies are found by searching the values of ω, giving vanishing eigenvalues of the inverse singlet linear response matrix ${}^1\boldsymbol{\chi}(\omega)^{-1} = \boldsymbol{\chi}_{IP}(\omega)^{-1} - {}^1\boldsymbol{\Xi}$, and the triplet excitation energies are found by searching the values of ω, giving vanishing eigenvalues of the inverse triplet linear response matrix ${}^3\boldsymbol{\chi}(\omega)^{-1} = \boldsymbol{\chi}_{IP}(\omega)^{-1} - {}^3\boldsymbol{\Xi}$. For $H_2$ in a minimal basis, ${}^1\boldsymbol{\chi}(\omega)^{-1}$ and ${}^3\boldsymbol{\chi}(\omega)^{-1}$ are $4 \times 4$ matrices that are block diagonal, the (oo,vv) block being uncoupled to the (ov,vo) block. For both singlet and triplet cases, the four positive poles of $\chi_{IP}(\omega)$ transform into four excitation energies (plus four symmetric deexcitation energies).

Between the two positive excitation energies coming from the (ov,vo) block of the matrix ${}^1\boldsymbol{\chi}(\omega)^{-1}$, the lowest one is identified with the first singlet ${}^1\Sigma_u^+$ excitation energy, which is called the optical gap. It is plotted in Figure 18.4 and compared with the reference FCI excitation energy and also with the fundamental gap $\mathcal{E}_2 - \mathcal{E}_1$ to highlight the effect of the Bethe–Salpeter kernel. At small internuclear distance, $R \leq 3$ Bohr, the Bethe–Salpeter kernel brings the BSE-GW curve very close to the FCI curve. For large $R$, the BSE-GW excitation energy follows the curve of the fundamental gap, which slightly overestimates the excitation energy at $R = 10$ Bohr but eventually goes to the correct limit $I - A$ when $R \to \infty$. Thus, contrary to the BSE-GW method using the noninteracting Green's function, the obtained excitation energy curve has now a

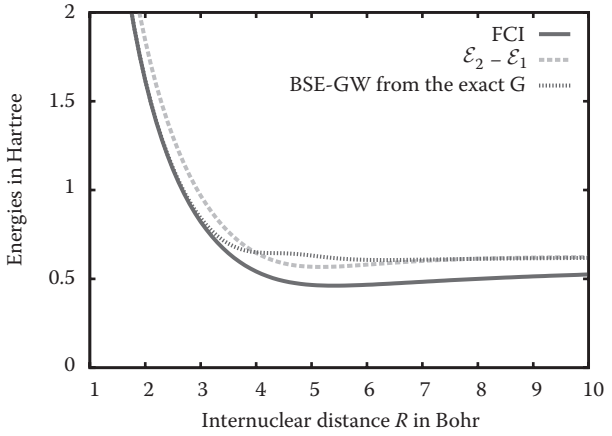


**FIGURE 18.4** Excitation energy of the singlet $^1\Sigma_u^+$ state of $H_2$ in a minimal basis as a function of the internuclear distance $R$ calculated by FCI and BSE-GW with the exact Green's function. The lowest pole of $\chi_{IP}(\omega)$, the fundamental gap $\mathcal{E}_2 - \mathcal{E}_1$, is also plotted for comparison.

correct shape. This relies on the fundamental gap being a good starting approximation to the optical gap. As regards the second excitation energy coming from the (ov,vo) block of the matrix $^1\boldsymbol{\chi}(\omega)^{-1}$, which is connected to the highest pole $\mathcal{E}_2' - \mathcal{E}_1'$ of $\chi_{IP}(\omega)$, it is a spurious excitation due to the approximate Bethe–Salpeter kernel used.

The lowest positive excitation energy coming from the (oo,vv) block of the matrix $^1\boldsymbol{\chi}(\omega)^{-1}$ is identified with the second singlet $^1\Sigma_g^+$ excited state that has a double excitation character. It is plotted in Figure 18.5 and compared with the FCI excitation

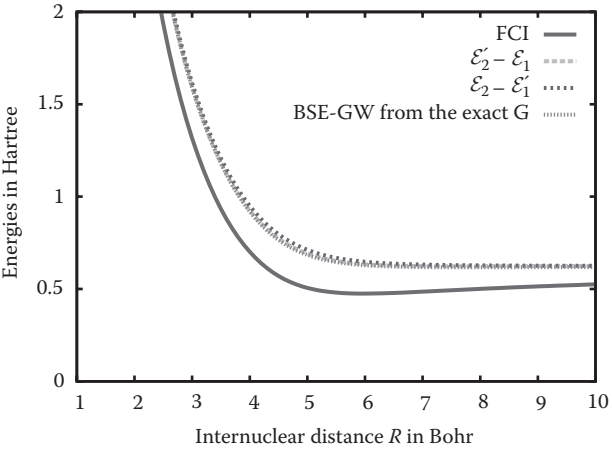


**FIGURE 18.5** Excitation energy of the second singlet $^1\Sigma_g^+$ state of $H_2$ in a minimal basis as a function of the internuclear distance $R$ calculated by FCI and BSE-GW with the exact Green's function. The poles $\mathcal{E}_2' - \mathcal{E}_1$ and $\mathcal{E}_2 - \mathcal{E}_1'$ of $\chi_{IP}(\omega)$ are also plotted for comparison.

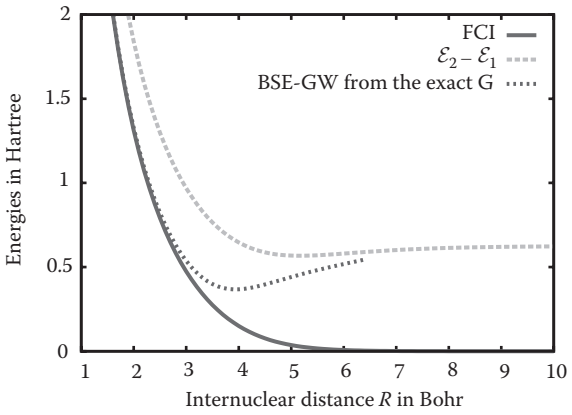


**FIGURE 18.6** Excitation energy of the triplet ${}^3\Sigma_u^+$ state of $H_2$ in a minimal basis as a function of the internuclear distance $R$ calculated by FCI and BSE-GW with the exact Green's function. The lowest pole of $\chi_{IP}(\omega)$, the fundamental gap $\mathcal{E}_2 - \mathcal{E}_1$, is also plotted for comparison.

energy for this state and with the poles $\mathcal{E}_2' - \mathcal{E}_1$ and $\mathcal{E}_2 - \mathcal{E}_1'$ of $\chi_{IP}(\omega)$. It is noteworthy that the BSE-GW method starting from $\chi_{IP}(\omega)$ instead of $\chi_0(\omega)$ but using a frequency-independent kernel does describe this double excitation state with an overall correct shape for the energy curve. However, the BSE-GW excitation energy is almost identical to the two poles $\mathcal{E}_2' - \mathcal{E}_1$ and $\mathcal{E}_2 - \mathcal{E}_1'$. The Bethe–Salpeter kernel in the static GW approximation thus brings virtually no improvement for this state over the starting poles of $\chi_{IP}(\omega)$. The (oo,vv) block of the matrix ${}^1\boldsymbol{\chi}(\omega)^{-1}$ also gives a second higher excitation energy that is spurious.

We finally consider the triplet excited state ${}^3\Sigma_u^+$. The lowest positive excitation energy coming from the (ov,vo) block of the matrix ${}^3\boldsymbol{\chi}(\omega)^{-1}$ should be identified with this state. It is plotted in Figure 18.6 and compared with the FCI excitation energy for this state and with the fundamental gap $\mathcal{E}_2 - \mathcal{E}_1$. For small internuclear distances, $R \leq 3$ Bohr, the BSE-GW method gives an accurate excitation energy, but for larger $R$, instead of going to zero, the BSE-GW excitation energy curve heads for the fundamental gap curve until the excitation energy becomes imaginary for $R \geq 6.5$ Bohr. The problem is that the poles of $\chi_{IP}(\omega)$ are the same for both singlet and triplet cases, and the fundamental gap $\mathcal{E}_2 - \mathcal{E}_1$ is not a good starting approximation to the triplet excitation energy in the dissociation limit. The Bethe–Salpeter kernel in the static GW approximation is not able to compensate for this bad starting point. In addition to this excitation energy, the BSE-GW method gives three other spurious triplet excitation energies.

## 18.5 CONCLUSION

We have applied the BSE approach in the static GW approximation for the calculation of the excitation energies on the toy model of $H_2$ in a minimal basis. We have tested two variants for the starting one-particle Green's function: the noninteracting HF one and the exact one. Around the equilibrium internuclear distance,

both variants give accurate excitation energies to the first singlet $^1\Sigma_u^+$ and triplet $^3\Sigma_u^+$ excited states. In the dissociation limit, however, the two variants differ. The first variant, starting from the noninteracting one-particle Green's function, badly fails in this limit for both singlet and triplet states, giving imaginary excitation energies. The second variant, starting from the exact one-particle Green's function, gives a qualitatively correct energy curve for the singlet $^1\Sigma_u^+$ excited state up to the dissociation limit. This relies on the fact that the fundamental gap (given by the one-particle Green's function) is a good starting approximation to the first singlet excitation energy. However, the same variant gives an incorrect energy curve for the triplet $^3\Sigma_u^+$ excited state in the dissociation limit. In this case, the fundamental gap is a bad starting approximation to the first triplet excitation energy.

The second BSE variant using the exact one-particle Green's function gives more excitation energies than the first BSE variant. Most of them are spurious excitations due to the approximate Bethe–Salpeter kernel used. However, one of them can be identified with the excitation energy to the singlet $^1\Sigma_g^+$ excited state that has a double excitation character. It is remarkable that such a double excitation can be described at all without using a frequency-dependent kernel. However, the Bethe–Salpeter kernel in the static GW approximation is insufficient to describe accurately the energy curve of this state, even around the equilibrium distance.

## ACKNOWLEDGMENTS

We thank L. Reining (École Polytechnique, Palaiseau, France) for suggesting to test the use of the exact one-particle Green's function in the BSE and F. Sottile (École Polytechnique, Palaiseau, France) and K. Pernal (Politechnika Łódzka, Łódź, Poland) for discussions.

## REFERENCES

1. Runge, E. and Gross, E. K. U., *Phys. Rev. Lett.*, 52, 997, 1984.
2. Gross, E. K. U. and Kohn, W., *Phys. Rev. Lett.*, 55, 2850, 1985.
3. Casida, M. E., in *Recent Advances in Density Functional Methods, Part I*, Chong, D. P., ed., World Scientific, Singapore, 1995, 155.
4. Petersilka, M., Gossmann, U. J., and Gross, E. K. U., *Phys. Rev. Lett.*, 76, 1212, 1996.
5. Dreuw, A., Weisman, J. L., and Head-Gordon, M., *J. Chem. Phys.*, 119, 2943, 2003.
6. Maitra, N. T., Zhang, F., Cave, R. J., and Burke, K., *J. Chem. Phys.*, 120, 5932, 2004.
7. Gritsenko, O. V., van Gisbergen, S. J. A., Görling, A., and Baerends, E. J., *J. Chem. Phys.*, 113, 8478, 2000.
8. Tawada, Y., Tsuneda, T., Yanagisawa, S., Yanai, T., and Hirao, K., *J. Chem. Phys.*, 120, 8425, 2004.
9. Kronik, L., Stein, T., Refaely-Abramson, S., and Baer, R., *J. Chem. Theory Comput.*, 8, 1515, 2012.
10. Casida, M. E., *J. Chem. Phys.*, 122, 054111, 2005.
11. Huix-Rotllant, M. and Casida M. E., http://arxiv.org/abs/1008.1478.
12. Pernal, K., Gritsenko, O., and Baerends, E. J., *Phys. Rev. A*, 75, 012506, 2007.
13. Pernal, K., Giesbertz, K., Gritsenko, O., and Baerends, E. J., *J. Chem. Phys.*, 127, 214101, 2007.

14. Giesbertz, K. J. H., Baerends, E. J., and Gritsenko, O. V., *Phys. Rev. Lett.*, 101, 033004, 2008.
15. Giesbertz, K. J. H., Pernal, K., Gritsenko, O. V., and Baerends, E. J., *J. Chem. Phys.*, 130, 114104, 2009.
16. Pernal, K., *J. Chem. Phys.*, 136, 184105, 2012.
17. Strinati, G., *Riv. Nuovo Cim.*, 11, 1, 1988.
18. Rohlfing, M. and Louie, S. G., *Phys. Rev. B*, 62, 4927, 2000.
19. Onida, G., Reining, L., and Rubio, A., *Rev. Mod. Phys.*, 74, 601, 2002.
20. Rohlfing, M., *Int. J. Quantum Chem.*, 80, 807, 2000.
21. Grossman, J. C., Rohlfing, M., Mitas, L., Louie, S. G., and Cohen, M. L., *Phys. Rev. Lett.*, 86, 472, 2001.
22. Tiago, M. L. and Chelikowsky, J. R., *Solid State Commun.*, 136, 333, 2005.
23. Hahn, P. H., Schmidt, W. G., and Bechstedt, F., *Phys. Rev. B*, 72, 245425, 2005.
24. Tiago, M. L. and Chelikowsky, J. R., *Phys. Rev. B*, 73, 205334, 2006.
25. Tiago, M. L., Kent, P. R. C., Hood, R. Q., and Reboredo, F. A., *J. Chem. Phys.*, 129, 084311, 2008.
26. Grüning, M., Marini, A., and Gonze, X., *Nano Lett.*, 9, 2820, 2009.
27. Ma, Y., Rohlfing, M., and Molteni, C., *Phys. Rev. B*, 80, 241405, 2009.
28. Ma, Y., Rohlfing, M., and Molteni, C., *J. Chem. Theory Comput.*, 6, 257, 2010.
29. Rocca, D., Lu, D., and Galli, G., *J. Chem. Phys.*, 133, 164109, 2010.
30. Grüning, M., Marini, A., and Gonze, X., *Comput. Mater. Sci.*, 50, 2148, 2011.
31. Blase, X. and Attaccalite, C., *Appl. Phys. Lett.*, 99, 171909, 2011.
32. Romaniello, P., Sangalli, D., Berger, J. A., Sottile, F., Molinari, L. G., Reining, L., and Onida, G., *J. Chem. Phys.*, 130, 044108, 2009.
33. Sangalli, D., Romaniello, P., Onida, G., and Marini, A., *J. Chem. Phys.*, 134, 034115, 2011.
34. Bruneval, F., Ph.D. thesis, Ecole Polytechnique, 2005.
35. Toulouse, J., Zhu, W., Ángyán, J. G., and Savin, A., *Phys. Rev. A*, 82, 032502, 2010.
36. Hedin, L., *Phys. Rev.*, 139, 1965.
37. Shirley, E. L. and Martin, R. M., *Phys. Rev. B*, 47, 15404, 1993.
38. Romaniello, P., Guyot, S., and Reining, L., *J. Chem. Phys.*, 131, 154111, 2009.
39. Toulouse, J., Zhu, W., Savin, A., Jansen, G., and Ángyán, J. G., *J. Chem. Phys.*, 135, 084119, 2011.
40. Ángyán, J. G., Liu, R.-F., Toulouse, J., and Jansen, G., *J. Chem. Theory Comput.*, 7, 3116, 2011.
41. Dewar, M. J. S. and Kelemen, J., *J. Chem. Educ.*, 48, 494, 1971.
42. Aryasetiawan, F., Gunnarsson, O., and Rubio, A., *Europhys. Lett.*, 57, 683, 2002.
43. Hirata, S. and Head-Gordon, M., *Chem. Phys. Lett.*, 314, 291, 1999.
44. Cai, Z.-L. and Reimers, J. R., *J. Chem. Phys.*, 112, 527, 2000.
45. Casida, M. E., Gutierrez, F., Guan, J., Gadea, F.-X., Salahub, D., and Daudey, J.-P., *J. Chem. Phys.*, 113, 7062, 2000.
46. Giesbertz, K. J. H. and Baerends, E. J., *Chem. Phys. Lett.*, 461, 338, 2008.